JOURNAL OF MATERIALS SCIENCE 23 (1988) 3992–3996

Stress intensity factors and CODs defined by in-plane displacements measured by scanning electron microscopy

P. S. THEOCARIS, C. A. STASSINAKIS, V. KYTOPOULOS
Department of Engineering Sciences, Athens National Technical University, PO Box 77230, Athens Gr175-10, Greece

A method is developed for evaluating the displacement field around the tip of a crack in a plate under plane stress or strain conditions by executing a number of measurements in this area through the scanning electron microscope. Several spots were created around the crack tip by using the electron beam of the SEM, which were used as reference points. A theory was developed which yields the components of the in-plane displacements and their differences from the coordinates of the reference spots measured through SEM. The method presents the advantage that its results are independent of the exact position of the crack tip and therefore it is suitable for performing measurements very close to this tip. Experimental evidence with plexiglas plates showed the validity of the method for defining the displacement field as well as the values of crack opening displacements and the stress intensity factor.

1. Introduction

One of the most interesting problems in fracture mechanics is the evaluation of the displacements around crack tips, which permits the computation of the respective stress intensity factor, and the crack opening displacement (COD) field along the crack flanks. The problem becomes more pronounced in the case of edge cracks where exact solutions do not exist. Thus, the development of an experimental technique to measure accurately these quantities around the crack tip is considered worthwhile.

Existing experimental methods are mainly based on the mechanical or optical interferometry methods. These techniques are the Moiré method [1, 2], the holographic Moiré method [3–6], the speckle interferometry method [7–9] and the SEM-stereoimaging method [10], while a few "isolated" methods, like those based on ultrasonic measurements [11] and special optoelectronic systems [12] could be also mentioned.

A common characteristic of the three methods based on interferometry is the indirect evaluation of the displacement field by means of a fringe pattern, which, especially for the case of the holographic Moiré method, is connected with the well-known difficulty in the unambiguous determination of the fringe orders.

Moreover, the first and second of the above methods have an additional handicap as they require the difficult construction on the specimen of highly accurate special high-frequency phase grating to achieve acceptable sensitivity. It must also be noted that the sensitivity of the third method is, in fact, limited by the optical apparatus, which does not permit accurate localization of the crack tip.

Furthermore, because the stress and displacement fields around the crack tip are rapidly changing with the polar distance from the crack tip and there is a strong variation of the thickness of the plate creating a dimple around the crack tip, the mode of evaluation of the displacements by the Moiré method and the holographic interferometry method, based on several neighbouring fringes, forcibly introduces a large error in the evaluation of displacements. Moreover, the lack of flatness in the vicinity of the crack tip is another source of error for all three optical methods.

On the other hand, the stereoscopic processing of photographs, which is connected with parallax errors and the poor magnification of photographs, considerably restricts the accuracy of the SEM-stereoimaging method. Finally, all the above methods are inherently connected with errors due to rigid body rotation.

In the method developed in this paper an experimental technique for the direct evaluation of the displacement field is developed, using scanning electron microscope measurements. Initially, the displacements, which are expressed in power series form [13], are analysed resulting in a system of linear equations, whose solution gives the whole displacement field around the crack-tip. In order to solve this linear system the relative displacements of only two arbitrary points are required, which can be readily achieved by scanning electron microscopy (SEM). In this way the evaluation of the displacement field can be performed, free from the errors and restrictions which influence the previously mentioned methods. It is shown in the paper that the computation of the displacement field and the evaluation of the stress intensity factor (SIF), as well as the determination of

0022–2461/88 $03.00 + .12

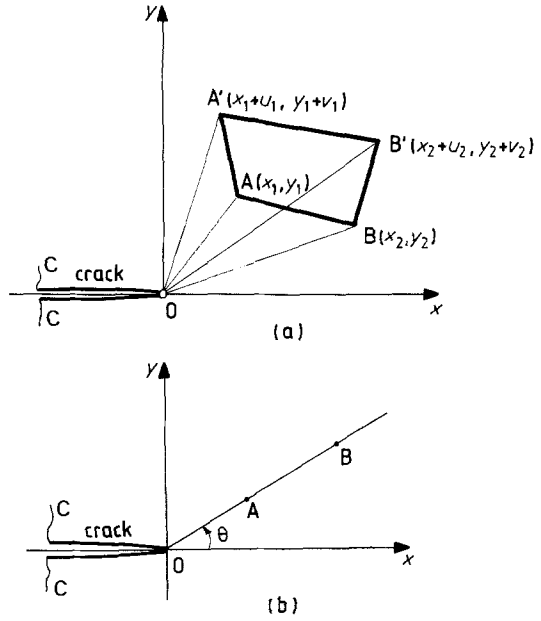

Figure 1(a, b) Geometry of an edge crack.

the crack shape under loading was achieved in an accurate manner by this technique.

2. Theoretical considerations

We consider an elastic body under plane stress conditions with finite dimensions containing an edge crack 0C, shown in Fig. 1a, and a system of coordinates $0xy$ with origin at the tip of the crack. We apply a stress σ_∞ at infinity of the plate and along the $0y$ axis. The generic points $A(x_1, y_1)$, $B(x_2, y_2)$ in the vicinity of the crack tip move during deformation to the new positions $A'(x_1 + u_1, y_1 + v_1)$, $B'(x_2 + u_2, y_2 + v_2)$ where u_1, v_1 and u_2, v_2 are the displacements of A and B, respectively.

The distance (A'B') is given by:

$$(A'B') = (x_2 + u_2 - x_1 - u_1)^2 + (y_2 + v_2 - y_1 - v_1)^2 \quad (1)$$

which, after some algebra, and introducing the relations

$$u_2 - u_1 = \Delta u, \quad v_2 - v_1 = \Delta v \quad (2)$$

yields

$$(A'B')^2 = (AB)^2 + (\Delta u)^2 + (\Delta v)^2 + 2(x_2 - x_1)\Delta u + 2(y_2 - y_1)\Delta v \quad (3)$$

Ignoring the terms $(\Delta u)^2$, $(\Delta v)^2$ in Equation 3, which are much smaller than the other terms for infinitesimal displacements, we derive

$$(A'B')^2 - (AB)^2 = 2(x_2 - x_1)\Delta u + 2(y_2 - y_1)\Delta v \quad (4)$$

Moreover, due to the infinitesimal displacements of points A, B we may assume that

$$(A'B') + (AB) = 2(AB) \quad (5)$$

and Equation 4 becomes

$$(AB) = \frac{x_2 - x_1}{(AB)}(\Delta u) + \frac{y_2 - y_1}{(AB)}(\Delta v) \quad (6)$$

If the polar coordinates for points A, B are (r_A, θ) and (r_B, θ), respectively, i.e. if these points are assumed along a polar radius from the crack tip (Fig. 1b), we have

$$\frac{x_2 - x_1}{(AB)} = \cos\theta, \quad \frac{y_2 - y_1}{(AB)} = \sin\theta \quad (7)$$

Thus, Equation 6 becomes

$$\Delta(AB) = (\Delta u)\cos\theta + (\Delta v)\sin\theta \quad (8)$$

On the other hand, the u, v-displacements for a given point for the problem under consideration are expressed by [13]

$$u(r, \theta) = \frac{1}{2\mu}\sum [r^{(n-1/2)} d_{2n-1} f_3(n, \theta) + r^n d_{2n} f_4(n, \theta)]\cos\theta - \frac{1}{2\mu}\sum [r^{(n-1/2)} d_{2n-1} f_1(n, \theta) + r^n d_{2n} f_2(n, \theta)]\sin\theta \quad (9)$$

$$v(r, \theta) = \frac{1}{\mu}\sum [r^{(n-1/2)} d_{2n-1} f_3(n, \theta) + r^n d_{2n} f_4(n, \theta)]\sin\theta + \frac{1}{\mu}\sum [r^{(n-1/2)} d_{2n-1} f_1(n, \theta) + r^n d_{2n} f_2(n, \theta)]\cos\theta \quad (10)$$

where

$$\begin{aligned} f_1(n, \theta) &= (-1)^n\left[(\tfrac{5}{2} + n - 4\sigma)\sin(n - \tfrac{3}{2})\theta - \left(\frac{2n-3}{2}\right)\sin(n + \tfrac{1}{2})\theta\right] \\ f_2(n, \theta) &= (-1)^n[(n - \sigma)\sin(n - 1)\theta - (n + 1)\sin(n + 1)\theta] \\ f_3(n, \theta) &= (-1)^n[(\tfrac{7}{2} - n - 4\sigma)\cos(n - \tfrac{3}{2})\theta + (n - \tfrac{3}{2})\cos(n + \tfrac{1}{2})\theta] \\ f_4(n, \theta) &= (-1)^{n+1}[(3 - n - 4\sigma)\cos(n - 1)\sigma + (n + 1)\cos(n + 1)\theta] \end{aligned} \quad (11)$$

In these relations μ is the shear modulus of the material, E is the elastic modulus, ν the Poisson ratio, and d_i unknown coefficients, whereas it is valid that $\sigma = \nu/(1 + \nu)$ for plane stress and $\sigma = \nu$ for plane strain. Applying Equation 9 at the points $A(r_A, \theta)$ and $B(r_B, \theta)$ and considering $\Delta u = (u_A - u_B)$, $\Delta v = (v_A - v_B)$ we derive the following equations

$$\Delta u = \frac{1}{2\mu}\sum [(r_A^{n-1/2} - r_B^{n-1/2}) d_{2n-1} f_3(n, \theta)\cos\theta + (r_A^n - r_B^n) d_{2n} f_4(n, \theta)\cos\theta] - \frac{1}{2\mu}\sum [(r_A^{n-1/2} - r_B^{n-1/2}) d_{2n-1} f_1(n, \theta)\sin\theta + (r_A^n - r_B^n) d_{2n} f_2(n, \theta)\sin\theta] \quad (12)$$

$$\Delta v = \frac{1}{\mu}\sum [(r_A^{n-1/2} - r_B^{n-1/2}) d_{2n-1} f_3(n, \theta) \sin\theta + (r_A^n - r_B^n) d_{2n} f_4(n, \theta) \sin\theta] + \frac{1}{\mu}\sum [(r_A^{n-1/2} - r_B^{n-1/2}) d_{2n-1} f_1(n, \theta) \cos\theta + (r_A^n - r_B^n) d_{2n} f_2(n, \theta) \cos\theta] \quad (13)$$

Introducing the values for Δu and Δv from these relations into Equation 8 we derive

$$\Delta(AB) = \frac{1}{2\mu}\sum d_{2n-1}(r_A^{n-1/2} - r_B^{n-1/2}) \times [f_3(n, \theta)\cos\theta - f_1(n, \theta)\sin\theta]\cos\theta + \frac{1}{2\mu}\sum d_{2n}(r_A^n - r_B^n)[f_4(n, \theta)\cos\theta - f_2(n, \theta)\sin\theta]\cos\theta + \frac{1}{2\mu}\sum d_{2n-1}(r_A^{n-1/2} - r_B^{n-1/2})[2f_3(n, \theta)\sin\theta + 2f_1(n, \theta)\cos\theta]\sin\theta + \frac{1}{2\mu}\sum d_{2n}(r_A^n - r_B^n)[2f_4(n, \theta)\sin\theta + 2f_2(n, \theta)\cos\theta]\sin\theta \quad (14)$$

Equation 14, after some straightforward algebra, may be written in the form

$$\sum d_{2n-1} t_1(n, r_A, r_B, \theta) + \sum d_{2n} t_2(n, r_A, r_B, \theta) = 2\mu\Delta(AB) \quad (15)$$

where the quantities t_1 and t_2 are expressed by

$$t_1(n, r_A, r_B, \theta) = (r_A^{n-1/2} - r_B^{n-1/2}) \times [f_3(n, \theta)(1 + \sin^2\theta) + f_1(n, \theta)\sin\theta\cos\theta] \quad (16)$$

and

$$t_2(n, r_A, r_B, \theta) = (r_A^n - r_B^n) \times [f_4(n, \theta)(1 + \sin^2\theta) + f_2(n, \theta)\cos\theta\sin\theta] \quad (17)$$

Equation 15 connects the unknown coefficients d_i ($i = 1, 2, \ldots, 2n$) with the already known quantities r_A, r_B, θ and $\Delta(AB)$. In the case where we consider $2n$ measurements for $\Delta(AB)$, we get $2n$ equations from Equation 15 consisting of a linear system of equations

$$\boldsymbol{AX} = \boldsymbol{B} \quad (18)$$

where

$$x_i = d_i \quad (i = 1, 2, \ldots, 2n) \quad (19)$$

are the elements of the vector $\boldsymbol{X}$, and

$$b_i = 2\mu\Delta(AB) \quad (i = 1, 2, \ldots, 2n) \quad (20)$$

are the elements of vector $\boldsymbol{B}$ and a_{ij} are the known elements of matrix $\boldsymbol{A}$, which take the values

$$a_{ij} = t_1\left(\frac{j+1}{2}, r_{A,i}, r_{B,i}, \theta_i\right)$$

with

$$i = 1, 2, 3, \ldots, 2n$$
$$j = 1, 3, 5, \ldots, 2n - 1 \quad (21)$$

and

$$a_{ij} = t_2\left(\frac{j}{2}, r_{A,i}, r_{B,i}, \theta_i\right)$$

with

$$i = 1, 2, 3, \ldots, 2n$$
$$j = 2, 4, 6, \ldots, 2n \quad (22)$$

Solving Equations 11 we can calculate the unknown coefficients of the terms of Equations 9 and 10 through which we may compute the displacements u, v in each point of the body.

3. Experimental results

In order to calculate the displacement field around the tip of an edge crack and the value of the stress intensity factor a series of experiments were done using the scanning electron microscope.

The microscope was the S4–10 scanning electron microscope made by Cambridge Scientific Instruments and the stereoscan tensile specimen stage, convenient to apply tensile loading to the tested specimens at different temperatures. SEM parameters were: beam voltage 20 kV, beam current 200 mA, filament current 3.5 A, jaw velocity varying 0.001 to 1.0 mm min^{-1} and maximum load capacity 2226 N.

The specimens were put in the tensile specimen stage of the microscope and submitted to a constant strain rate $\dot{\varepsilon} = 1.3 \times 10^{-3}$ sec^{-1}. In each step of loading the crack tip zones were photographed, using a magnification factor from 200 to 1000.

The specimens were made from Plexiglas plates with the following mechanical properties: shear modulus $\mu = 125 \times 10^7$ N m^{-2} and Poisson ratio $\nu = 0.30$, while the dimensions of the specimens were: length $l = 35$ mm, width $w = 6$ mm, thickness $d = 2$ mm. Natural edge cracks were formed in the specimens by using a fatigue procedure with lengths varying from 0.4 to 1.5 mm.

All specimens were coated with an aluminium coating to prevent charging effects on their surface from the high voltage of the electron beam. On the other hand, by using the electron beam a series of spots in radial directions were created on the surface of the specimens (see Fig. 2). The direct measurement of the distance between two neighbouring spots in two successive steps of load, permits the computation of the quantity $\Delta(AB)$ in Equation 15. In each test 20 to 30 such measurements were performed. Hence, from Equation 18 the coefficients of the series given in Equations 9 and 10 were computed and finally the displacements u, v for every point in the plane were evaluated. Moreover, the stress intensity factor can be computed from these measurements because it is related with the coefficient of the first term of the series expansion in Equations 9 and 10.

The experimental results for the displacements u, v are plotted in Figs 3 and 4, for various angles θ from

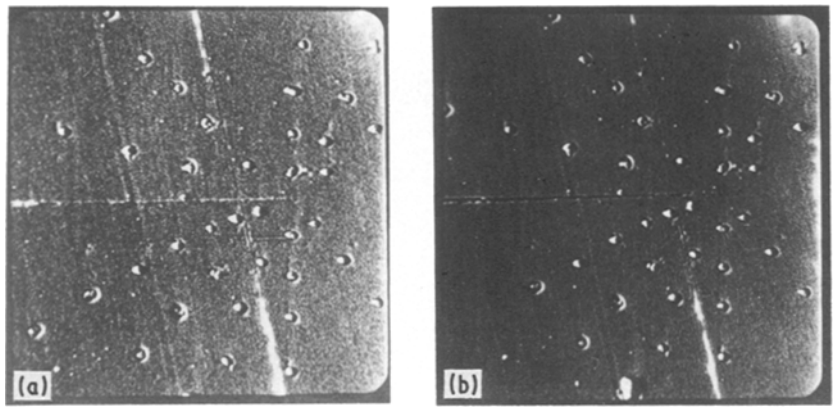

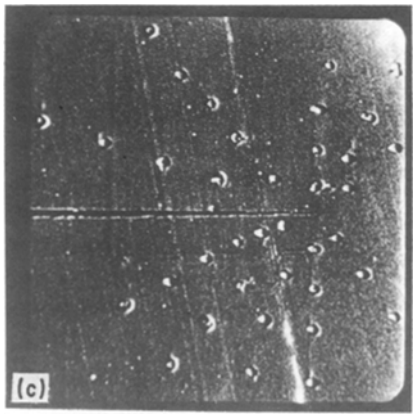

Figure 2 Series of photographs showing the shape of the crack under different loads.

0° to 180° and for various distances for the crack-tip 0, normalized to the distance a, equal to the edge-crack length. It is seen that the v-displacements increase with angle θ and distance from the crack tip, with the largest values of v at $\theta = 180°$ corresponding to the crack lips. On the contrary, u-displacements present maximum values at $\theta = 0°$ and decrease with this angle, reaching negative values for $\theta = 180°$. This means that the lips of the crack having $u < 0$ behave in a way resulting in a shortening of the crack length. With known values of u, v for $\theta = 180°$ the shape of the crack under loading may be reconstructed as given in Fig. 5, which almost coincides with an elliptical form.

The values of SIF as determined from the coefficient of the first term of the series are given in Fig. 6, together with their approximate values obtained for the same geometry and loading from Gray [14], and Bowie [15]. It is apparent from this figure that the experimental data and the theoretical approximations are in good agreement.

4. Discussion

In the present paper the displacement field around the crack-tip and the corresponding SIF were computed by means of direct measurements performed in the SEM.

The advantage of the present method lies in the fact that the measurements made during the tests are independent of any coordinate system. This independence

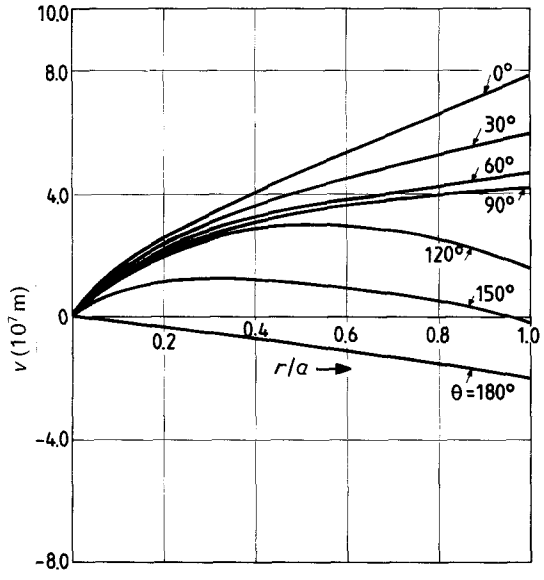

Figure 3 Variation of u-displacement with r/a ratio.

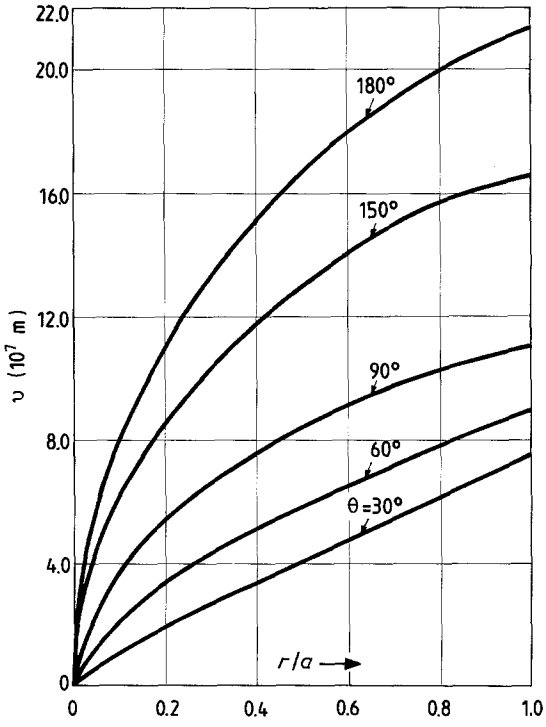

Figure 4 Variation of v-displacement with r/a ratio.

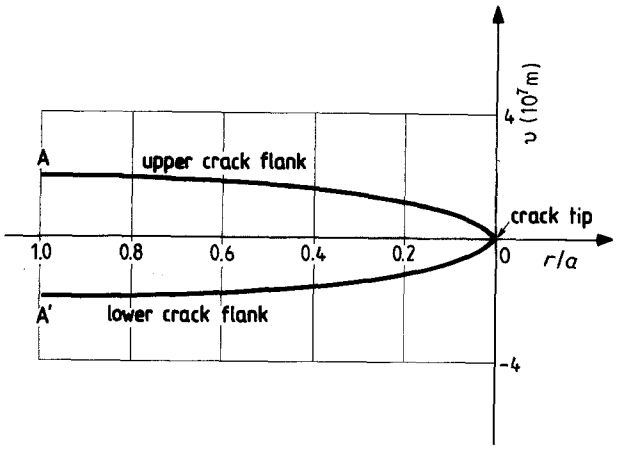

Figure 5 The shape of a loaded edge crack.

contributes significantly to the accuracy of the method in evaluating elastic, and particularly, plastic displacements, because, as is known, the crack-tip moves during loading, resulting in erroneous measurements related to an absolute coordinate system.

In addition, the decoupling of measurements from any coordinate system, permits high magnifications to be used and high accuracy to be achieved in the evaluation of distances between given points. The same property also allows the performance of measurements in the close vicinity of the crack-tip, an area which is normally forbidden for other experimental methods.

The results presented in this paper yield information concerning especially crack-opening displacements at the crack tips, thus permitting the exact definition of the crack shape under loading. In addition, experimental evaluation of SIF showed good agreement with existing approximate methods. This evaluation may be executed either from the definition of the factor of the first term in the series expansion, or, and perhaps much better, through the values of CODs accurately defined along the crack tips.

References

1. P. S. THEOCARIS, Moiré Fringes in Stain Analysis (Pergamon, Oxford, 1969).
2. R. E. LINK and R. J. SANFORD, "Micro-Moiré–a High Sensitivity Moiré Technique for Determining Displacement Fields by Using Phase Gratings as Amplitude Gratings", Proceedings of the 1985 SEM, Spring Conference on Experimental Mechanics, (Soc. for Exp. Mech. Publ., Connecticut, 1985).
3. D. B. BARKER, R. J. SANFORD and R. CHONA, *Exp. Mech.* (1985) 399.
4. W. J. DALLY, C. A. SCIAMMARELLA and J. SHAREEF, "Determination of Stress Intensity Factor K_I from In-plane Displacement Measurements", Proceedings of the Vth International Congress on Experimental Mechanics (1984) p. 122.

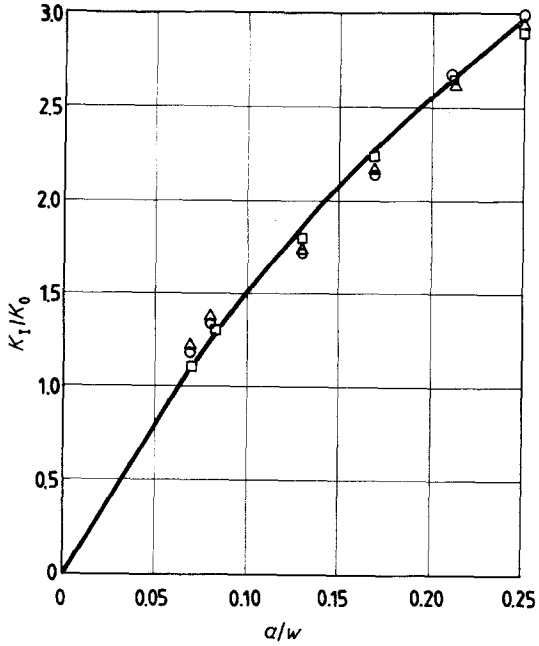

Figure 6 The variation of SIF with a/w ratio. (△) [14], (○) [15], (□) present work.

5. P. D. PLOTKOWSKI, "Separation of Displacement Components in Holographic Interferometry by Use of A Carrier Fringe Technique", Proceedings of the 1985 SEM, Spring Conference on Experimental Mechanics, (Soc. Exp. Mech. Publ., Connecticut, 1985) p. 676.
6. D. POST and R. CZARNEK, "Holographic Interferometry: Error Caused by Thermal Gradients in Holographic Plates", Proceedings of the V International Congress on Experimental Mechanics, (Soc. Exp. Mech. Publ., Connecticut, 1984) p. 506.
7. W. T. EVANS and A. LUXMOORE, *Engng Fract. Mech.* **5** (1974) 735.
8. F. A. AMIN and W. T. EVANS, *J. Strain Anal.* **9** (1) (1974) 32.
9. E. ARCHOLD and J. BURCH, *Optica Acta* **17** (1970) 883.
10. D. L. DAVIDSON, "The Observation and Measurement of Displacements and Strain by Stereoimaging", in "Scanning Electron Microscopy" (SEM Inc., AMF O'Hare, Jl 60666, USA, 1979) p. 79.
11. M. A. HAMED and T. C. CHU, "Ultrasonic Displacement Measurement Using Digital Correlation", Proceedings of the 1985 SEM, Spring Conference on Experimental Mechanics, (Soc. Exp. Mech. Publ., Connecticut, 1985) p. 819.
12. C. A. SCIAMARELLA and M. AHMADSHAHI, "A Optoelectronic System for Fringe Pattern Analysis", *ibid.*, p. 861.
13. B. GROSS, E. ROBERTS and J. SRAWLEY, *Int. J. Fract. Mech.* **4** (1969) 267.
14. T. G. F. GRAY, *Int. J. Fract.* **13** (1977) 65.
15. O. L. BOWIE, in "Methods of Analysis and Solutions of Crack Problems", Vol. I, edited by G. C. Sih (Noordhoff, The Hague, 1977) pp. 1–55.

Received 5 October 1987
and accepted 26 January 1988